Vapor-Phase Thermal Conductivity, Vapor Pressure, and Liquid Density of R365mfc

Isabel M. Marrucho,[†] Nelson S. Oliveira,[†] and Ralf Dohrn*,[‡]

Departamento de Química, Universidade de Aveiro, P-3810−193 Aveiro, Portugal, and Process Technology, Fluid Properties and Thermodynamics, Bayer, Building B310, D-51368 Leverkusen, Germany

The thermal conductivity of a new fluoroalkane, R365mfc (1,1,1,3,3-pentafluorobutane), important for the production of polyurethane rigid foams, was measured using a transient hot wire method, at temperatures between 336.85 K and 377.4 K. The extended corresponding states theory was used successfully to predict the results, with an average absolute deviation of 0.5%. The vapor pressure (302.90 K to 358.15 K) and the liquid density (289.15 K to 413.15 K, at pressures up to 9.85 MPa), were measured, using the dynamic method and the vibrating tube method, respectively. The critical point of R365mfc, required for the thermal conductivity calculations, was calculated with the correlations of Dohrn (*J. Supercrit. Fluids* **1992**, *5*, 81) using the normal boiling point and the liquid density at 20 °C as input data.

1. Introduction

Due to its high insulating capacity, rigid polyurethane (PUR) foam is used in a large number of different applications. It is usually produced from a two-component system: component A contains polyol, including catalysts, stabilizers, and blowing agents, and component B is a polyisocyanate. Since the reaction between the diisocyanate and the diol is highly exothermic, it is possible to use inert, low-boiling liquids and/or water as blowing agents. Water reacts with the polyisocyanate to form carbon dioxide (CO_2) which serves as an additional blowing agent. These physical blowing agents vaporize during polymerization, and are trapped in bubbles or cells formed by the polymer. Blowing agents with a high vapor pressure increase the pressure in the foam cells which leads to a higher mechanical stability of the foam at a given foam density. A higher foam stability could be used for a reduction of the density (e.g., from 35 kg·m^{-3} to 30 kg·m^{-3}), leading to considerable savings of raw material (polyisocyanate and polyol). The thermal conductivity of the cell gas is responsible for 60% to 65% of the heat transfer through the foam, that is important for the properties as an insulating material. Due to its low vapor-phase thermal conductivity (10.5 mW·m^{-1}·K^{-1} at 355.65 K), CFC-11 has been the most widely used blowing agent until recently. The fact is that due to the high stability of the CFCs, they reach the ozone layer before being destroyed by a natural process.[1] To find adequate substitutes for CFC-11, the vapor-phase thermal conductivity of several potential blowing agents has been measured. Today, mixtures (e.g., cyclopentane + isopentane) formulated to combine the best of both worlds, low thermal conductivity and high vapor pressure at low temperatures, have been introduced into the market. The goal of our investigations is to gain a better understanding of the relevant practical properties of market blowing agents and to obtain basic data for the modeling of the foaming process, which is of great importance for the quality of the foam and for the economics of foam production.

The focus of the present paper is R365mfc and its application as a blowing agent. For that purpose, the vapor-phase thermal conductivity, the vapor pressure, and the liquid density have been measured. The critical point has been predicted and the acentric factor has been determined using its definition by Pitzer[8] from the experimental vapor-pressure data and the predicted critical point.
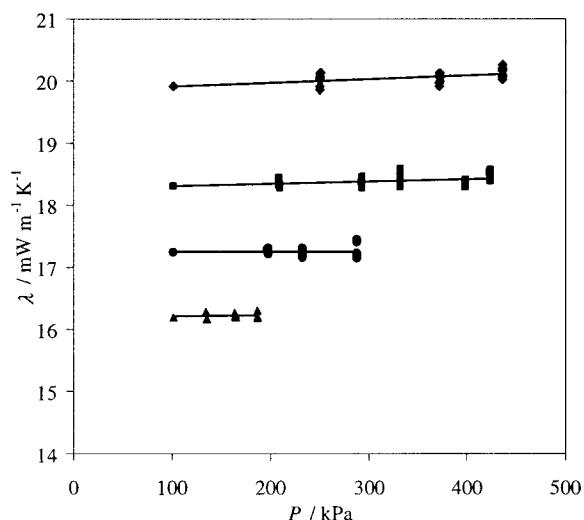
2. Experimental Section

The experimental thermal conductivity measurements were carried out in an apparatus based on the transient hot wire method, which is the IUPAC reference method.[2] An overview of the development and technical details of the measurements of the thermal conductivity of gases has been given.[2,3] The measuring cell[4] (stainless steel, 1.4571) with a length of 267 mm and a diameter of 48 mm consists of two parallel chambers with platinum wires of different lengths (ratio of lengths ≈ 0.28) and 10 μm of diameter. The second wire was used to compensate the end effects. The temperature was controlled with an air thermostat within ±0.1 K. The temperature was measured using calibrated PT 100 resistance thermometers with an uncertainty within ±0.1 K, which might lead to an error of ±0.01 mW·m^{-1}·K^{-1} or 0.06% for the thermal conductivity of R365mfc. More information on the apparatus has been given elsewhere.[4] All pressure sensors used for the measurements of the thermal conductivity, the vapor pressure and the liquid density were transducers from Keller. They were calibrated using a pressure balance (DESGRANGES ET HUOT; Druckblock 410, Typ 26000 M, Terminal 20000). The uncertainty of the pressure measurement is within ±0.1 kPa.
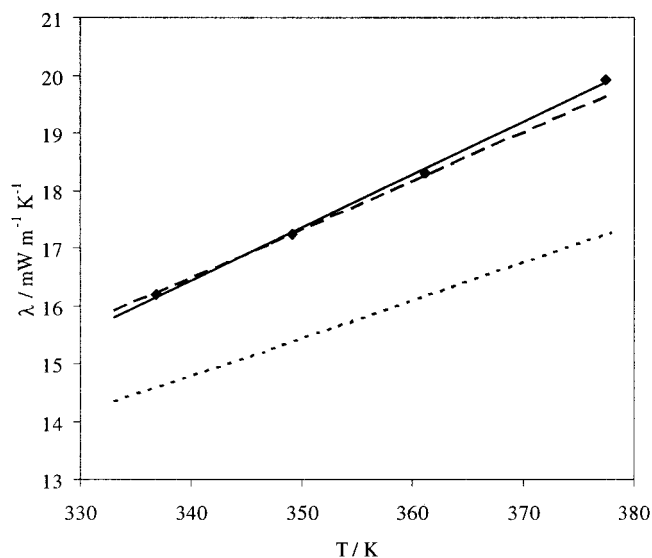
The essential feature of the transient hot-wire method is the precise determination of the transient temperature with a thin metallic wire. This is determined from measurements of the resistance of the wire over a period of few seconds followed by the initiation of the heating cycle, with a $\Delta T = (2.000 \pm 0.025)$ K. Immediately after the heating, the same wires work as resistance thermometer incorporated in the arms of a Wheatstone bridge. In this work, several corrections to the ideal transient hot wire

* To whom correspondence should addressed. E-mail: ralf.dohrn. rd@bayer-ag.de. Fax: ++49−214−30−81554.
† Universidade de Aveiro.
‡ Bayer.

Table 1. Vapor-Phase Thermal Conductivity, λ, of R365mfc from 336.85 K to 377.40 K with Data Points at 101.3 kPa Being Extrapolated Values

T = 336.85 K		T = 349.13 K		T = 361'.14 K		T = 377.40 K	
P	λ	P	λ	P	λ	P	λ
kPa	mW·m⁻¹·K⁻¹	kPa	mW·m⁻¹·K⁻¹	kPa	mW·m⁻¹·K⁻¹	kPa	mW·m⁻¹·K⁻¹
101.3	16.20	101.3	17.24	101.3	18.30	101.3	19.92
134.7	16.27	197.0	17.24	208.6	18.44	250.1	19.91
134.9	16.16	197.2	17.29	208.6	18.31	250.1	20.02
163.5	16.21	197.2	17.27	208.8	18.40	250.1	20.04
163.6	16.26	197.6	17.31	208.9	18.33	250.1	20.08
163.9	16.20	197.9	17.21	209.0	18.30	250.1	20.12
164.0	16.19	198.3	17.27	209.2	18.33	250.2	19.91
164.0	16.20	231.9	17.26	209.3	18.28	250.2	20.05
164.1	16.23	231.9	17.27	292.8	18.37	250.3	19.86
186.1	16.19	231.9	17.15	293.0	18.33	250.8	20.14
186.3	16.30	231.9	17.26	293.2	18.28	372.2	20.13
186.3	16.20	232.0	17.22	293.2	18.43	372.3	19.91
186.4	16.18	232.0	17.22	293.3	18.36	372.3	19.98
186.7	16.20	232.1	17.29	293.3	18.45	372.4	20.00
		232.1	17.18	293.5	18.34	372.4	20.06
		232.3	17.30	331.8	18.37	372.5	20.12
		287.9	17.22	331.9	18.30	436.3	20.20
		288.0	17.17	331.9	18.47	436.3	20.10
		288.1	17.15	332.1	18.38	436.3	20.16
		288.2	17.14	332.1	18.55	436.3	20.06
		288.2	17.40	332.1	18.44	436.4	20.10
		288.3	17.45	332.3	18.58	436.4	20.03
				398.6	18.30	436.4	20.10
				398.6	18.39	436.4	20.08
				398.9	18.36	436.5	20.26
				399.0	18.41	436.6	20.19
				399.41	18.31		
				399.4	18.36		
				423.4	18.53		
				423.7	18.57		
				423.8	18.38		
				423.9	18.42		
				424.0	18.46		
				424.0	18.49		

Figure 1. Vapor-phase thermal conductivity of R365mfc: ♦, *T* = 377.40 K; ■, *T* = 361.14 K; ●, *T* = 349.13 K; ▲, *T* = 336.85 K.

Figure 2. Temperature dependence of the experimental and predicted with ECST thermal conductivity for R365mfc at 101.3 kPa: ♦, experimental data; −, linear correlation; − −, ECST with f_{int} from eq 4; ···, ECST with $f_{int} = 1.32 \times 10^{-3}$.

method[4] were made. These corrections can be divided in two main sources: corrections due the wire and due to the existence of an outer isothermal boundary layer. In the first correction the finite radius of the wire (5 μm) is accounted for, which produces a short-time temperature lag relative to the ideal model. The second correction accounts for the penetration of the fluid temperature gradient to the outer cell wall which leads to the transition from transient conduction into an infinite medium to steady-state conduction in a concentric cylindrical region. At lower pressures

the linear region in the temperature rise versus the logarithm of elapsed time is reduced. This is due to the high thermal diffusivity of the gas, which is inversely proportional to the gas density. For the low-density region, the use of a steady-state method with a transient hot-wire apparatus has been proposed.[5] In this work, experiments were performed in the transient state. The lowest pressures
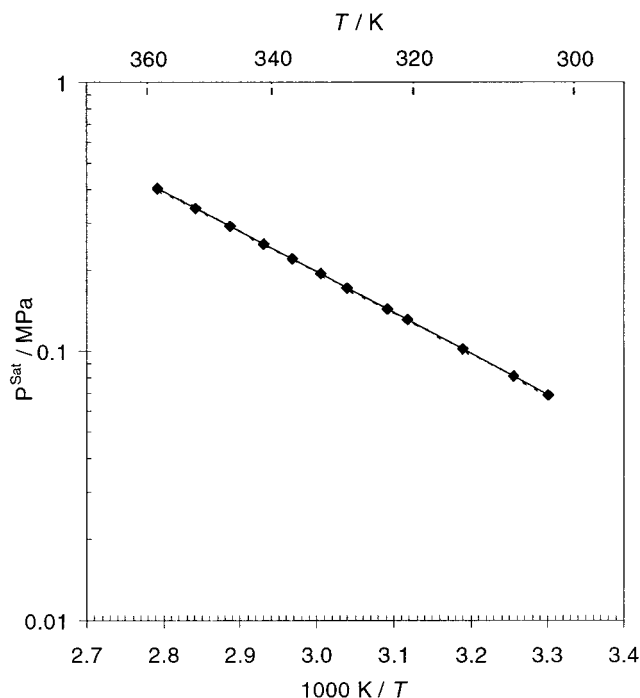
Figure 3. Vapor pressure of R365mfc: ◆, experimental data; −, Wagner equation (eq 7); ···, Antoine Equation (eq 6).

Table 2. Vapor Pressure, P^{Sat}, of R365mfc from 302.90 K to 358.15 K

T	P^{Sat}
K	MPa
302.90	0.0685
307.20	0.0806
313.46	0.1016
320.67	0.1308
323.45	0.1437
328.95	0.1721
332.80	0.1945
336.94	0.2209
341.10	0.2501
346.37	0.2916
351.97	0.3409
358.15	0.4027

of the measurements were selected to give a sufficiently large linear portion to obtain reliable results for the slope of the temperature rise versus logarithm of time. For each temperature, between 40 and 80 individual data points were taken at different pressures.

Before starting the thermal conductivity measurements with R365mfc, the accuracy of the apparatus was checked by measuring the thermal conductivity of carbon dioxide at two temperatures. The values obtained are in excellent agreement (relative difference of ±0.03%) with the IUPAC recommended reference values.[6] The uncertainty at the level of 95% confidence of the experimental data, including the extrapolation of the data to atmospheric pressure, is estimated to be within ±3%.

The vapor pressure and the liquid density of R365mfc were also measured. For the vapor-pressure measurements, a double-walled glass apparatus based on the dynamic method was used for temperatures between 293 K and 373 K. The vapor pressure was measured by determining the boiling temperature of the sample at various known pressures. A cartridge heater, which is inserted into the glass apparatus from below, was used for heating the liquid sample. Using a Cottrell pump the boiling liquid is recirculated. The temperature sensor is a

Table 3. Liquid Density, ρ, of R365mfc from 289.15 K to 413.15 K at Different Pressures

T	P	ρ	T	P	ρ
K	MPa	kg·m^{-3}	K	MPa	kg·m^{-3}
289.15	0.039	1273.4	353.15	0.352	1128.2
	0.109	1273.5		0.358	1128.2
	2.115	1278.0		2.067	1136.2
	4.199	1282.5		4.098	1145.0
	6.051	1286.5		6.037	1152.9
	8.042	1290.5		8.018	1160.5
	9.562	1293.5		9.853	1167.1
293.40	0.047	1264.7	373.15	0.584	1074.6
	0.097	1264.8		0.603	1074.6
	2.055	1269.5		2.016	1083.5
	4.033	1273.9		4.015	1095.1
	6.136	1278.6		6.000	1105.5
	8.145	1282.8		8.026	1115.3
	9.553	1285.6		9.825	1123.3
313.15	0.100	1223.2	393.15	0.909	1013.8
	0.137	1223.3		0.947	1014.1
	2.025	1228.6		2.001	1023.8
	4.063	1234.2		4.007	1040.1
	6.069	1239.5		6.048	1054.4
	8.063	1244.6		8.010	1066.6
	9.765	1248.7		9.816	1078.7
333.15	0.197	1177.4	413.15	1.339	941.9
	0.210	1177.4		1.416	943.0
	2.028	1184.0		2.051	952.6
	4.020	1190.0		4.066	977.8
	6.051	1197.5		6.008	997.0
	8.007	1203.5		8.030	1013.9
	9.745	1208.6		9.818	1027.3

100 Ω Platinum resistance thermometer, calibrated by PTB (Physikalisch-Technische Bundesanstalt, Braunschweig, Germany) according to the ITS-90 convention. The uncertainty of the temperature measurement is ±0.02 K. The temperature constancy at a constant pressure indicates that the boiling point has been reached. After the vapor−liquid equilibrium has been reached, the temperature is taken to be the boiling temperature for the given pressure. Then, the pressure is raised and the next point on the vapor-pressure curve is taken. The apparatus has been used to measure vapor-pressure curves of several hundred components. The uncertainty of the vapor-pressure measurement is estimated to be within ±0.2%.

For the liquid density measurements the vibrating tube method was used. It basically consists on the determination of the vibration frequency of a U-tube which is filled with the liquid of interest. The vibration frequency changes according to the additional mass of the tube due to the fluid. For the calibration of the apparatus, water was used. Its vibration time was measured at normal temperature, as well as the vibration time for vacuum. The vibration time for the desired substance at the desired temperature is then measured, as well as the vibration time for vacuum at the same temperature. A densimeter Anton PAAR DM60/DM601 has been used for the experiments. The pressure could be adjusted using a screw pump from vacuum up to 40 MPa. The temperature was controlled by a thermostatic bath within ±0.1 K. The temperature was measured using a calibrated PT 100 resistance thermometer with an uncertainty within ±0.1 K. The uncertainty of the density measurement is less than ±0.2%.

R365 mfc was purchased from Solvay with a purity of >99.5%. Before the experiments the material was degassed by reboiling it under vacuum.

3. Extended Corresponding States Theory

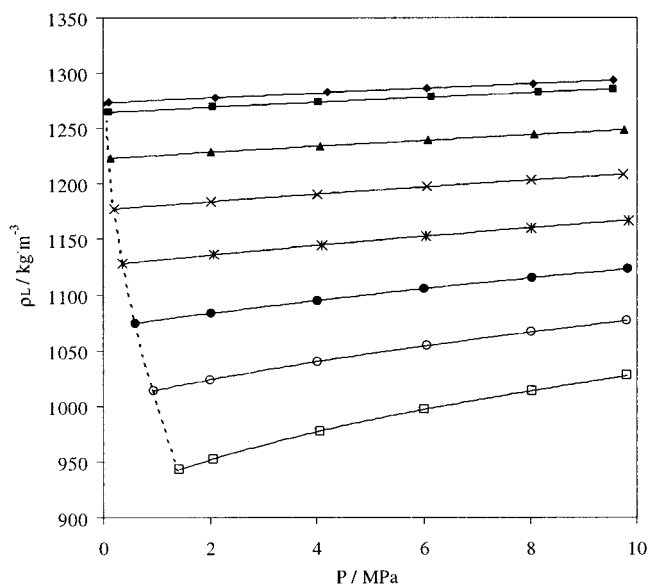The thermal conductivity at 101.3 kPa was predicted using the Extended Corresponding States Theory (ECST)

Figure 4. Liquid density of R365mfc: $\blacklozenge$, $T = 289.15$ K; $\blacksquare$, $T = 293.40$ K; $\blacktriangle$, $T = 313.15$ K; $\times$, $T = 333.15$ K; $*$, $T = 353.15$ K; $\bullet$, $T = 373.15$ K; $\circ$, $T = 393.15$ K; $\square$, $T = 413.15$ K; $--$, saturation line.

according to the formalism of Ely and Hanley,[7] where the thermal conductivity is considered to be a summation of two terms: one arising from the transfer of energy due translational effects, λ^{trans}, and the other due the internal degrees of freedom, λ^{int}. Thus

$$\lambda(\rho, T) = \lambda^{trans}(\rho, T) + \lambda^{int}(T) \tag{1}$$

The contribution to λ^{trans} is expressed as a sum of a low-density contribution, λ^*, and a density-dependent contribution, λ^+

$$\lambda^{trans}(\rho, T) = \lambda^*(T) + \lambda^+(\rho, T) \tag{2}$$

The exact equations to calculate these contributions have been derived before.[7−9] It was observed that the density-dependent translational contribution, $\lambda^+(\rho, T)$, is almost negligible for the thermal conductivity of low-pressure gases (below few tenths of a percent), and the shape factors could be set to unity. The term $\lambda^{int}(T)$ has the dominating role in the thermal conductivity of low-pressure gases value. It is usually calculated using the modified Eucken correction for polyatomic gases[10]

$$\lambda^{int} = \frac{f_{int}\eta^*}{M}\left(C_p^{\,id} - \frac{5R}{2}\right) \tag{3}$$

where η^* is the dilute-gas viscosity, which can be estimated from kinetic theory, C_p^{id} the constant pressure ideal gas heat capacity, R the universal gas constant, and f_{int} a proportionality factor. In this work, C_p^{id} was calculated using Joback's group-contribution method.[9] In the original Eucken correlation f_{int} is constant and equal to 1×10^{-3} when R and C_p^{id} are in J·mol^{-1}·K^{-1}, η^* is in μPa·s, M is in g·mol^{-1}, and λ is in W·m^{-1}·K^{-1}. Huber and Ely[6] used the value 1.32×10^{-3}. In this work, the thermal conductivity was first calculated using $f_{int} = 1.32 \times 10^{-3}$ and then with the relationship suggested by Chapman and Cowling[11]

$$f_{int} = \frac{M\rho D}{\eta} \tag{4}$$

where D is the self-diffusion coefficient calculated by the

Table 4. Saturated Liquid Density, ρ^{Sat}, of R365mfc from 289.15 K to 413.15 K[a]

$\dfrac{T}{\text{K}}$	$\dfrac{P^{Sat}}{\text{MPa}}$	$\dfrac{\rho^{Sat}}{\text{kg·m}^{-3}}$
289.15	0.039	1273.4
293.40	0.047	1264.7
313.15	0.100	1223.2
333.15	0.197	1177.4
353.15	0.352	1128.2
373.15	0.584	1074.6
393.15	0.909	1013.8
413.15	1.339	941.9

[a] The vapor pressure, P^{Sat}, was calculated using eq 7.

Lee and Thodos correlation.[12] From the analysis of Figure 2, it can be observed that the results are superior when eq 4 is used (root-mean-square deviation: 0.148 mW·m^{-1}·K^{-1}) as compared to a calculation with $f_{int} = 1.32 \times 10^{-3}$ (root-mean-square deviation: 2.11 mW·m^{-1}·K^{-1}).

4. Results

4.1. Thermal Conductivity. The thermal conductivity of the vapor phase of R365mfc has been measured at four different temperatures between 336.85 K and 377.4 K and at pressures up to 0.438 MPa. The results are listed in Table 1 and plotted in Figure 1. The performance of PUR blowing agents concerning thermal conductivity is usually compared for a pressure of 101.3 kPa. Therefore it is a standard procedure for all blowing agents measured at Bayer to fit the isothermal data by a linear correlation to find the thermal conductivity at 101.3 kPa, even though for R365mfc the pressure dependence is low. The thermal conductivity at atmospheric pressure is shown in Figure 2. These data was correlated with a simple linear equation

$$\frac{\lambda}{\text{mW·m}^{-1}\text{·K}^{-1}} = A\frac{T}{\text{K}} + B \tag{5}$$

with $A = 0.091697$ and $B = 14.741$. The root-mean-square deviation between the experimental data at atmospheric pressure and eq 6 is 0.056 mW·m^{-1}·K^{-1}. Since there are no data in the literature for R365mfc, comparisons could not be made. Also in Figure 2, two lines for the prediction of the thermal conductivity of R365mfc using ECST are given.

4.2. Vapor Pressure and Liquid Density. In Table 2 the experimental results for the vapor pressure, P^{Sat}, are shown. The data have been correlated using the Antoine equation

$$\ln\left(\frac{P^{Sat}}{\text{MPa}}\right) = A - \frac{B}{T/\text{K} + C} \tag{6}$$

with $A = 7.35303$, $B = 2585.6565$ and $C = -45.2146$ and using the Wagner equation

$$\frac{P^{Sat}}{P_C} = \exp\left[\left(\frac{1}{1 - \tau}\right)(A\tau + B\tau^{3/2} + C\tau^3 + D\tau^6)\right] \tag{7}$$

with

$$\tau = 1 - \frac{T}{T_C} \tag{8}$$

and $A = -5.5153587$, $B = -1.5091145$, $C = -3.4278599$, and $D = 11.4082904$. It can be observed in Figure 3 that
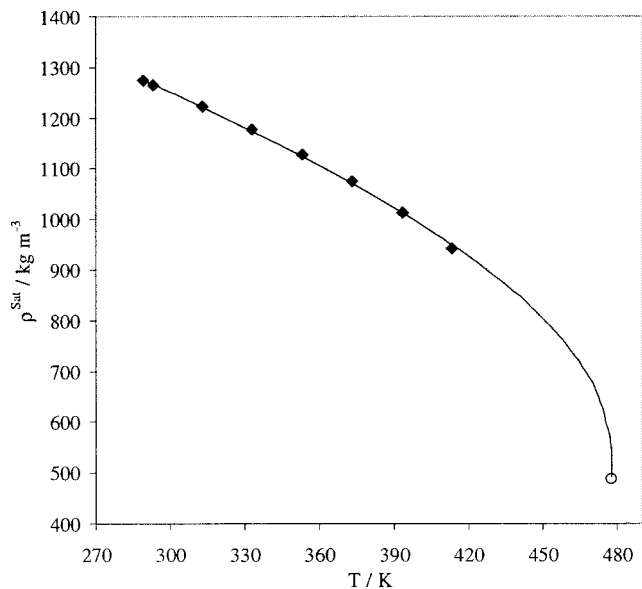
Figure 5. Saturated liquid density of R365mfc: ◆, experimental data; —, modified Rackett equation (eq 9); ○, critical point (calculated).

eq 6 (AAD = 0.039%) and eq 7 (AAD = 0.034%) both give a very good fit for R365mfc in the investigated temperature range.

Table 3 and Figure 4 show the experimental results for the liquid density of R365mfc at different temperatures and pressures. The saturated liquid density of R365mfc is given in Table 4. It was correlated with the modified Rackett equation

$$\frac{\rho}{\text{kg·m}^{-3}} = \frac{M}{\dfrac{RT_C}{P_C} A^{(1+(1-T_r)^B)}} \qquad (9)$$

with $A = 0.266486$ and $B = 0.34284$.

The critical point of R365mfc was calculated with the correlations of Dohrn[13,14] using the coefficients for halogenated compounds. As input data the normal boiling point and the liquid density at 20 °C of R365mfc were used. The following results for the critical temperature, T_C, and the critical pressure, P_C, were obtained:

$$T_C = 477.7 \text{ K}$$

$$P_C = 3.489 \text{ MPa}$$

These values were used in eq 7 to describe the vapor-pressure curve and in eq 9 to describe the saturated liquid density. From the measured vapor-pressure data and the calculated critical point, the acentric factor ω can be determined using its definition by Pitzer,[8] which leads to

$$\omega = 0.233$$

$$\rho_C = 488 \text{ kg·m}^{-3}$$

The critical density ρ_C was calculated from the critical compressibility using ω and three-parameter corresponding states tables.[9] The uncertainty is estimated[14] to be within ±1.5% for T_C, ±2.5% for P_C, and ±4% for the acentric factor. Figure 5 depicts the saturated liquid density data including the critical point and the correlation using the modified Rackett equation (eq 9). The root-mean-square deviation is 3.8 kg·m⁻³.

Literature Cited

(1) Hong, S.-U.; Duda, J. L. Diffusion of CFC 11 and hydrofluorocarbons in polyurethane. *J. Appl. Polym. Sci.* **1998**, *70*, 2069−2073.
(2) Assael, M. J.; Nieto de Castro, C. A.; Roder, H. M.; Wakeham, W. A. *Measurement of the Transport-Properties of Fluids*; Wakeham, W. A., Nagashima, A., Sengers, J. V., Ed.; Blackwell: Oxford, England, 1991.
(3) Johns, A. I.; Scott, A. C.; Watson, J. T. R.; Ferguson, D.; Clifford, A. A. Measurements of the thermal conductivity of gases by the transient hot-wire method. *Philos. Trans. R. Soc. London A* **1988**, *325*, 295−365.
(4) Dohrn, R.; Treckmann, R.; Heinemann, T. Vapor-phase thermal conductivity of 1,1,2,2-pentafluoropropane, 1,1,1,3,3-pentafluoropropane, 1,1,2,2,3-pentafluoropropane and carbon dioxide. *Fluid Phase Equilib.* **1999**, *158−160*, 1021−1028.
(5) Roder, H. M.; Perkins, R. A.; Leasecke, A.; Nieto de Castro, C. A. Absolute steady-state thermal conductivity measurements by use of a transient hot-wire system. *J. Res. Nat. Inst. Stand. Technol.* **2000**, *105*, 221−253.
(6) Vesovic, V.; Wakeham, W. A., The transport properties of carbon dioxide. *J. Phys. Chem. Ref. Data* **1990**, *19*, 763−808.
(7) Ely, J. F.; Hanley, J. M. Prediction of Transport Properties. 2. Thermal Conductivity of Pure Fluids and Mixtures. *Ind. Eng. Chem. Fundam.* **1983**, *22*, 90−96.
(8) Huber, M. L.; Friend, D. G.; Ely, J. F. Prediction of the Thermal Conductivity of Refrigerants and Refrigerant Mixtures. *Fluid Phase Equilib.* **1992**, *80*, 249−261.
(9) Reid, R.; Prausnitz, J. M.; Poling, B. E. *The Properties of Gases and Liquids*, 4th ed.; McGraw-Hill: New York, 1998.
(10) Hirschfelder, J. O.; Curtiss, C. F.; Bird, R. B. *Molecular theory of gases and liquids*; John Wiley and Sons Inc.: New York, 1967.
(11) Chapman, S.; Cowling, T. G. *The Mathematical theory of non-uniform gases*; Cambridge: New York, 1961.
(12) Lee, H.; Thodos, G. Generalized Treatment of Self-Diffusivity for the Gaseous and Liquid States of Fluids. *Ind. Eng. Chem. Fundam.* **1983**, *22*, 17−26.
(13) Dohrn, R. General Correlations for Pure-Component Parameters of Two-Parameter Equations of State. *J. Supercrit. Fluids* **1992**, *5*, 81−90.
(14) Dohrn, R. *Berechnung von Phasengleichwichten*; Vieweg-Verlag: Wiesbaden, Germany, 1994.